The Super-TIGER Scintillating Fiber Hodoscope

J. E. WARD [1], W. R. BINNS [1], R. G. BOSE [1], T. J. BRANDT [3], D. L. BRAUN [1], W. M. DANIELS [3], G. A. DE NOLFO [3], P. F. DOWKONTT [1], S. P. FITZSIMMONS [3], D. J. HAHNE [3], T. HAMS [3,6], M. H. ISRAEL [1], J. KLEMIC [2], A. W. LABRADOR [2], J. T. LINK [3,6], R. A. MEWALDT [2], J. W. MITCHELL [3], P. R. MOORE [1], R. P. MURPHY [1], M. A. OLEVITCH [1], B. F. RAUCH [1], K. SAKAI [3,6], F. SAN SEBASTIAN [3], M. SASAKI [3,6], G. E. SIMBURGER [1], E. C. STONE [2], C. J. WADDINGTON [4], M. E. WIEDENBECK [5]

[1] *Washington University, St. Louis, MO 63130 USA.*
[2] *California Institute of Technology, Pasadena, CA 91125 USA.*
[3] *NASA/Goddard Space Flight Center, Greenbelt, MD 20771 USA.*
[4] *University of Minnesota, Minneapolis, MN 55455 USA.*
[5] *Jet Propulsion Laboratory, California Institute of Technology, Pasadena, CA 91109 USA.*
[6] *Center for Research and Exploration in Space Science and Technology (CRESST), Greenbelt, MD 20771 USA.*

jward@physics.wustl.edu

Abstract: Super-TIGER is a large-area (5.4 m^2) instrument that was successfully launched from Antarctica in December 2012. It was designed to measure the abundances of cosmic-ray nuclei in the charge interval $30 \leq Z \leq 42$ with individual-element resolution and high statistical precision, and make exploratory measurements through Z = 56. It has also collected a large volume of data to measure with high statistical accuracy the energy spectra of the more abundant elements in the charge interval $10 \leq Z \leq 28$ at energies $0.8 < E < 10$ GeV/nucleon. Super-TIGER, which builds on the heritage of the smaller TIGER experiment, used a scintillating fiber hodoscope system to determine the straight-line trajectory of cosmic-ray particles incident on the instrument. This information allows for corrections for particle incident angle and detector area non-uniformities. A description of the hodoscope system along with details of the hodoscope's flight performance are presented.

Keywords: Super-TIGER, cosmic rays, OB associations, hodoscope.

1 Introduction

Super-TIGER (Super Trans-Iron Galactic Element Recorder [1] [2]), which builds on the legacy of the smaller TIGER experiment [3], is designed to measure cosmic-ray nuclei in the charge interval $30 \leq Z \leq 42$ with individual-element resolution and high statistical precision. It will also measure with high statistical accuracy the energy spectra of the more abundant elements in the interval $10 \leq Z \leq 28$ at energies $0.8 < E < 10$ GeV/nucleon. These measurements will help in the understanding of galactic cosmic-ray acceleration and origin [4] [5], along with a test of the hypothesis that micro-quasars may distort the otherwise smooth energy spectra [6]. Super-TIGER was launched on a Long Duration Balloon (LDB) from Williams Field, Antarctica on December 9th, 2012. It flew successfully for a NASA record-breaking LDB flight duration of 55 days.

Like TIGER, this instrument made use of scintillating fiber hodoscopes [7] to measure the trajectory of incident cosmic-ray particles. Measuring these trajectories allows corrections to be made to the measured particle signals for incident angle variation and instrument non-uniformities. These corrections are essential for achieving individual element resolution. Details of the hodoscope fiber fabrication, construction, electronics design and testing along with some preliminary aspects of in-flight performance will be discussed.

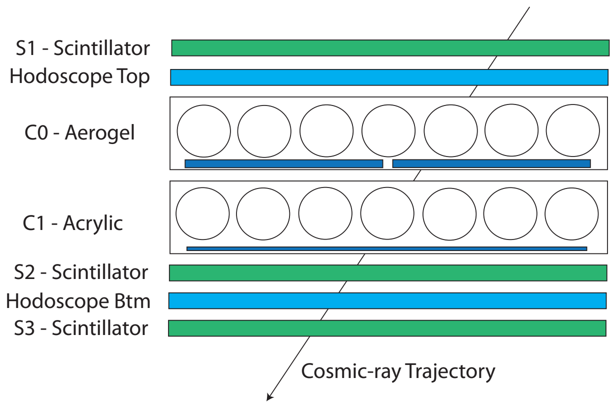

Figure 1: Cross section of a single Super-TIGER module.

2 Hodoscope Description

Super-TIGER consists of two detector stacks (modules) each with fiducial areas of 2.4 m × 1.16 m. There are four hodoscope planes employed in the overall design (two in each module, one bottom and one top, see Figure 1). Each plane consists of one "long" hodoscope layer (length 2.4 m, width 1.16 m) providing a transverse or "y" direction measurement with two "short" hodoscope layers (length and width 1.16 m) providing a longitudinal or "x" direction measurement (see Figure 2).

Each long hodoscope layer contains a total of $\sim$ 828 1.4 mm square cross-section fibers, with contiguous groups of 6 fibers organized into a "tab" and 12 tabs organized into a coarse "segment". For each short layer, there is a total of $\sim$ 1160 1.0 mm square cross-section fibers, with contiguous groups of 8 fibers organized into a tab and 12 tabs to a segment. Each tab is approximately 8 mm wide,

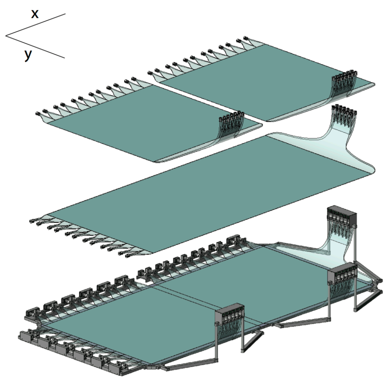

Figure 2: Top Image: Exploded view of the short and long hodoscope layers. Bottom Image: Combination of the layers coupled with the aluminum frame and PMT support brackets; this is a bottom plane configuration.

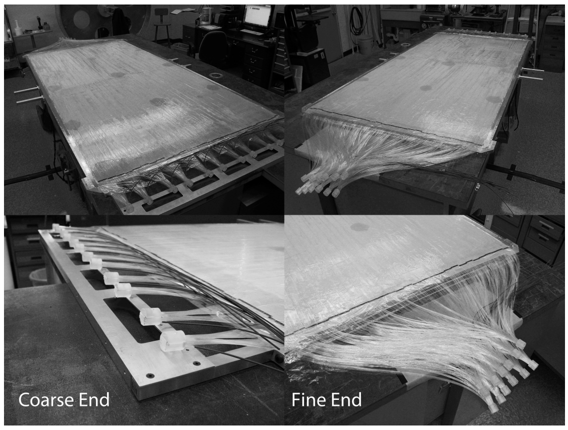

Figure 3: Photographs of a long hodoscope layer, both the coarse and fine ends.

and there are 12 segments for both the short and long layers.

Each fiber is made of a polystyrene plastic with scintillator dyes mixed in (primary butyl-PBD and secondary dimethly-POPOP, 1 % and 0.02 % by mass respectively) and surrounded by a $\sim$ 0.04 mm thick acrylic cladding.

As a particle traverses a fiber it excites the polystyrene molecules in the fiber core. These molecules then transfer energy via a non-radiative mechanism to the primary dye, which radiates this excess energy as ultra-violet light. This light is then collected by the secondary dye and re-radiated at blue wavelengths, where it is light-piped down the fiber to a Photo-Multiplier Tube (PMT) [8].

The maximum distances that this light will have to travel to a PMT range from 2 meters for the short fibers to 3.2 meters for the long fibers. These distances are in contrast to the original TIGER instrument which flew hodoscopes where the maximum light-transmission distances were 1.9 meters. The extra light attenuation expected due to this greater fiber length on Super-TIGER was compensated for by increasing the fiber cross-section for the long-layer fibers to 1.4 mm, thus reducing reflection losses.

Super-TIGER has 12 PMTs for the coarse and fine ends of each hodoscope layer, where each of the 12 segments goes to an individual coarse-end PMT, while a single tab from each segment goes to a separate fine-end PMT (see Figure 3 for a view of the fiber groupings and Section 4 for further discussion). Each PMT signal is digitized by a 14-bit pulse height analyzer located on the hodoscope front end electronics (FEE) board. For more information on the details of the hodoscope construction, please refer to [7].

2.1 Fiber Production and Testing

The Super-TIGER hodoscope fibers are drawn from heated boules ($\sim$ 3.8 cm square cross-section, clad with $\sim$ 1.58 mm thick acrylic) of the polystyrene/scintillator dye mixture over a large, slow-rotation aluminum wheel. A fiber is drawn until a ribbon of fibers is created, glued together with an elastomeric adhesive (Arathane 5753), and then cut at the required length. These ribbons are then laid out to make a hodoscope layer, with the ends finally formatted into the relevant tabs and segments.

As the minimum particle detection requirement for the hodoscope system is to successfully detect particles with at least charge Z = 10, it is important to verify that the fabricated fibers allow enough scintillation light to travel the full fiber distances to the PMTs and be successfully detected. This evaluation is carried out by attenuation tests using a Strontium-90 (Sr-90) electron source. The source is placed next to a test fiber at various locations along its length with the emitted scintillation light then collected by a PMT at one fiber end.

Previous studies show that there are approximately 80 times more pe's expected from a Z = 10 particle than from an Sr-90 source, thus giving >50 pe's for a particle passing at the furthest possible distance from the PMT. This is a large enough signal for detection and digitization by the front-end electronics.

2.2 Detectors and Electronics

As each hodoscope layer needs 12 PMTs for both the coarse and fine ends, there was a total of 288 hodoscope PMTs flown on Super-TIGER. The chosen PMT model is a Hamamatsu R1924A, which was selected due to its good quantum efficiency for blue light, relative cost and previously successful use on TIGER. PMTs with a high gain were pre-selected for use with the long hodoscope layers to further reduce the issue of attenuation of scintillation light signals for particles arriving at the maximum possible distance from a PMT.

The 12 PMTs on each hodoscope side are provided with high voltage (HV) by 2 HV trim boards (using EMCO CA12P 1250V power supplies), and are read out by a single hodoscope FEE board. The HV trim boards are a further development on the TIGER electronics system, allowing remote-controlled HV settings on individual PMTs.

Each PMT uses a custom linear-base circuit, which has undergone a visual and thermal testing procedure. The thermal procedure involves each PMT base being supplied with 1250 V and kept in an oven at 60° C for 24 hours. The voltages and currents are monitored to ensure no failure of any of the circuit components. After this "burn-in" procedure, each base is matched with a PMT and flashed with a blue LED for liveness and stability checks.

Once this procedure is finished, 12 PMTs and bases are potted with an RTV compound (RTV 627) and attached to the HV trim and hodoscope FEE boards (also potted using both an epoxy (50-3150 RFR) and RTV compound). The PMTs and boards are then put through a thermal (thermal cycling between -35°C and +55°C at 4 hours a cycle) and vacuum test procedure where the PMTs are again flashed with a blue LED and read out by the electronics systems for verification of the system liveness and stability during the environmental stresses. All the hodoscope PMTs functioned properly throughout the 55-day flight.

3 Hodoscope Plane Mapping

3.1 Methodology

The relative position of each fiber tab along the length of a hodoscope layer must be known to within $\sim$ 1.0 mm to ensure the most accurate measurement of the particle's trajectory through the instrument. This accuracy is vital in maintaining a good charge resolution in the final data analysis.

To achieve this, each hodoscope layer is secured to a testing bench with a motorized camera set-up placed above the layer. This set-up has transverse (x) and longitudinal (y) directional motors, allowing a downward-facing camera mounted on an arm to access a large majority of the fiducial area of the fiber layer. The set-up also consists of graduated rulers in both directions of motion, allowing a measurement of an individual fiber position to a 0.5 mm accuracy.

For the first fiber in each of the 12 segments of a layer, several points along its length are measured using the motorized system and camera and logged. These values are then used to generate a map of the fibers as they lay on the hodoscope substrate. Corrections of each fiber relative to the first segment fiber have been conducted, to account for segment to segment variations along the length of the hodoscope layers. This measurement procedure was repeated for each individual layer.

4 Trajectory Assignment

To determine the arrival and exit point of a particle in the instrument, Super-TIGER uses a hodoscope coding scheme similar to TIGER [9] whereby 144 fiber tabs on a layer can be read out by 12 fine and 12 coarse PMTs (see Figure 4 for an illustration of the hodoscope coding scheme). Each of the 12 segments go to the 12 coarse PMTs, while the Nth tab in each segment goes to the Nth fine-end PMT (i.e. the 1st tab in each of the 12 segments goes to the 1st PMT, the 2nd tab in each segment goes to the 2nd PMT etc.). Therefore, a particle can pass through a segment, lighting up the relevant coarse-end PMT (hence initially localizing the incident position to a segment width of 96 mm). A finer measurement can then be made by determining which fine-end PMT provided a signal (i.e. to within $\sim$ 8 mm).

With the combination of the x and y directional hodoscope layers, equation 1 can then be used to determine the trajectory angle θ (with respect to normal) of the particle through the instrument. Equation 1 is given as:

$$\sec(\theta) = \frac{(\mathrm{h}^2 + \mathrm{dx}^2 + \mathrm{dy}^2)^{\frac{1}{2}}}{\mathrm{h}} \tag{1}$$

where dx is the difference between tab positions in the top and bottom x-direction hodoscope layers, dy is the difference between tab positions in the top and bottom y-direction hodoscope layers and h is the distance separating the top and bottom hodoscope planes.

4.1 Contribution to Charge Resolution

The charge resolution depends on the hodoscope's accurate determination of the particle's path-length through the instrument. The uncertainty in the measurement of the incident angle θ relates to the charge resolution as follows [10]:

$$\sigma_z = \left(\frac{1}{\mathrm{n}\sqrt{6}}\right) \sin\theta\cos\theta \left(\frac{\mathrm{s}}{\mathrm{h}}\right) \mathrm{Z} \tag{2}$$

where n = 1.67 for scintillator signals $\propto Z^{1.67}$ [11] or n = 2 for Cherenkov signals $\propto Z^2$, s is the tab width, h is the height between top and bottom hodoscope planes and Z is the charge of the nucleus.

Thus, given an incident Zr particle (Z = 40) passing through the scintillator and using the value of $\sin\theta\cos\theta$ averaged over the effective instrument geometric factor ($<\sin\theta\cos\theta> = 0.38$), the hodoscope contribution in quadrature to the overall charge resolution is a negligible $\sim$ 0.003 cu. The contribution given a Cherenkov signal (n = 2) is even smaller.

5 Flight Performance

Super-TIGER collected data on over 60 million cosmic-ray events. The paths for $\sim$ 80% of the highest priority events (i.e. $\sim Z \geq 22$) were successfully reconstructed using the hodoscopes on both Super-TIGER modules. By requiring a good signal in eight PMTs (one on each end of 4 layers), 80% represents $\sim$ 97.25% efficiency in each of these eight signals.

The hit distributions in the x and y directions for Module 1 are shown in Figure 5 for all events collected between December 15th 2012 and January 29th 2013. The hodoscopes for both modules performed to expectations throughout the flight and are expected to be re-furbished and flown on any future Super-TIGER flights. The efficiency against time of the hodoscopes for high-priority charges is also shown in Figure 6.

5.1 Relative Signal Event Recovery

As a typical Super-TIGER event requires four layer "hits" to provide a particle's trajectory through the instrument, any missed layer means that the trajectory cannot be reconstructed using the hit implementation alone and must hence be removed from the analysis. Considering the rare nature of ultra-heavy cosmic rays, efforts are underway to recover events due to missing hits, thus improving the hodoscope's efficiency. One initial study currently underway is to use the relative signals from hit hodoscope fibers to estimate the position in a layer where there was no coarse hit (perhaps due to the particle traversing the fiber cladding as opposed to the central polystyrene plastic/scintillator dye core). Figure 7 shows a distribution of high-Z events (with a preliminary estimate of charge) where the coarse Y-coordinate estimate, using only the relative PMT signals, is compared against the "true" Y-coordinate measurement using the measured particle position. The resolution for the higher-charge events is $\sim$ 5.2 cm, which should prove effective in event recovery, although the study is in a preliminary phase.

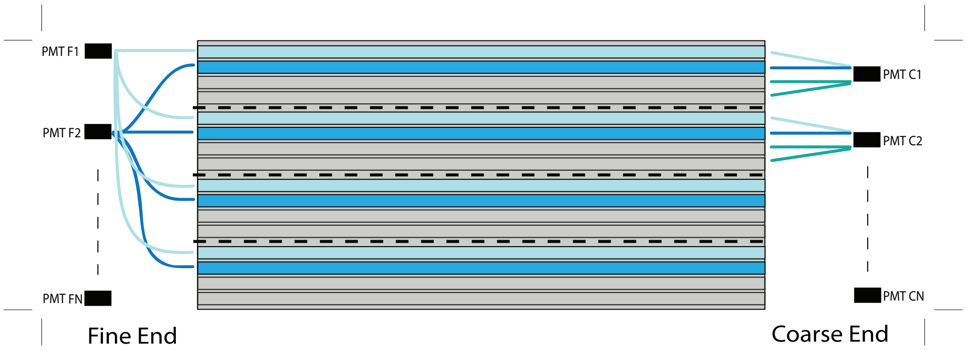

Figure 4: Illustration of the hodoscope coding system showing the fine and coarse ends of a layer (a long hodoscope layer in this example). The dashed lines designate individual segments, with only four tabs to a segment for clarity.

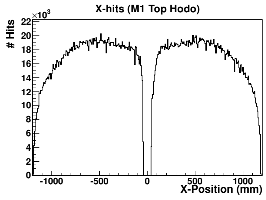

(a) X-position hits for the top hodoscope.

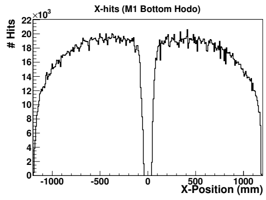

(b) X-position hits for the bottom hodoscope.

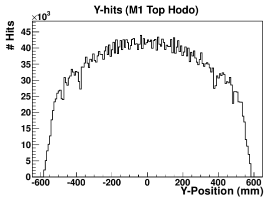

(c) Y-position hits for the top hodoscope.

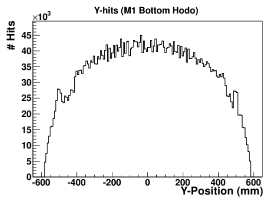

(d) Y-position hits for the bottom hodoscope.

Figure 5: Distribution of hodoscope hits for Module 1.

6 Conclusion

Scintillating fiber hodoscopes were fabricated, integrated and flown successfully on the Super-TIGER LDB flight in Antarctica in the 2012/2013 season. The hodoscopes performed to a high standard during the entire duration of the flight, ensuring the ability to apply angle and mapping corrections to the full Super-TIGER dataset.

Acknowledgment: This research at Washington University is supported by NASA under grant number NNX09AC17G and the McDonnell Center for the Space Sciences, Washington University in Saint Louis. We wish to thank the Columbia Scientific Balloon Facility (CSBF) personnel and the Wallops Balloon Program Office (BPO) for their excellent efforts that resulted in our highly successful long-duration balloon flight. We also wish to thank the National Science Foundation Office of Polar Programs for their outstanding logistical support which made this investigation possible.

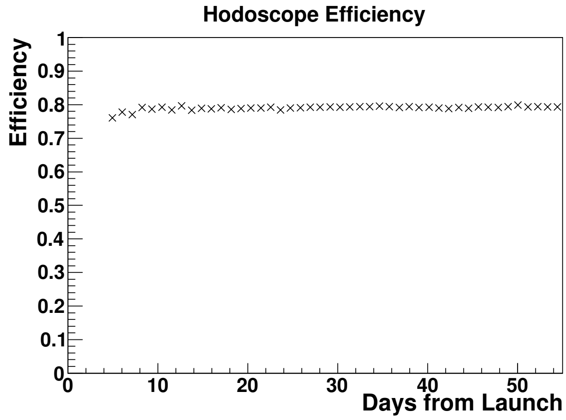

Figure 6: Hodoscope Efficiency for high-priority events over the majority of the flight duration.

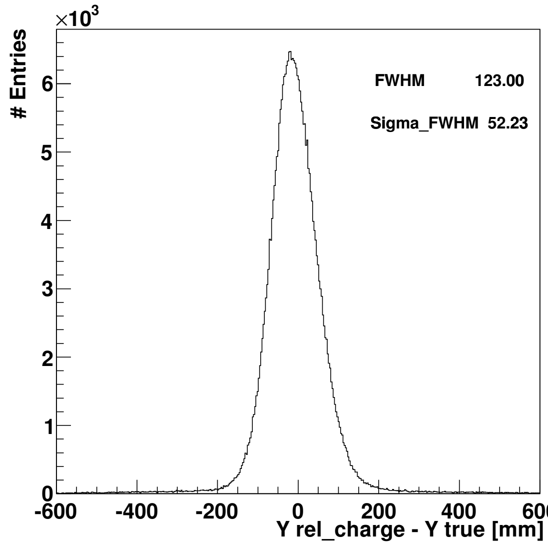

Figure 7: Relative-charge method distribution for charges in the range $30 \leq Z \leq 40$.

References

[1] Binns W. R., et al., *these proceedings*, ID 0645
[2] Mitchell, J. W., et al., ICRC 2011: Beijing, 2011, ID 1234
[3] Rauch, B. F., et al., ApJ, 2009, **697**: 2083-2088
[4] Higdon, J. C., Lingenfelter, R. E., ApJ, 2003, **590**: 822-832
[5] Binns, W. R., et al., ApJ, 2005, **634**: 351-364
[6] Heinz, S., Sunyaev, R., A&A, 2002, **390**: 751-766
[7] Ward, J. E., et al., ICRC 2011: Beijing, 2011, ID 0714
[8] Davis, A. J., et al., NIM, 1989, **276**: 347-358
[9] Lawrence, D. J., et al., NIM, 1999, **420**: 402-415
[10] Love, P. L., et al., NIM, 1977, **140**: 469-576
[11] Link, J. T., et al., ICRC 2011: Beijing, 2011, ID 737